Effect of Linear Density on the Mechanical Properties of 3D Spacer Composites with Improved Manufacturing Quality

Melisa Dincer[a,b], Emir Karci[a], Ibrahim Halil Sahin[a,c], Cagin Emre[a,c], Basak Ozkendirci[d], Elif Ozden Yenigun[e], Hulya Cebeci[a,b,c,*]

[a] *Aerospace Research Center, Istanbul Technical University, Istanbul, 34469, Turkey*
[b] *Aviation Institute, Istanbul Technical University, Istanbul, 34469, Turkey*
[c] *Department of Aeronautical and Astronautical Engineering, Istanbul Technical University, Istanbul, 34469, Turkey*
[d] *Faculty of Arts and Design, Department of Textile and Fashion Design, Dogus University, Istanbul, 34437, Turkey*
[e] *School of Design Textiles, Royal College of Art, SW7 2EU, London, United Kingdom*
**Corresponding author, hulya.cebeci@itu.edu.tr*

ABSTRACT

The innovative 3D weaving method allows I-beams to be woven in one piece and promises to eliminate delamination failure with the interlacing yarns. Therefore, woven I-beam composites have been developed to improve the resistance of laminated I-beam composite structures against delamination. In this study, woven I-beam fabrics (IBFs) were produced by the 3D weaving method by using 300, 600, and 1200 TEX E-glass fibers with a custom-built weaving machine. Then, IBFs were made into woven I-beam composites (IBCs) using the vacuum infusion method (VIP) to examine the influence of linear density on the mechanical properties of IBCs. The results of the three-point bending test represent that 300 TEX, 600 TEX (warp density: 20 ends/cm), 600 TEX (warp density: 12 ends/cm), and 1200 TEX samples had an average maximum flexural stress of 8.6, 9.2, 8.5, and 8.8 MPa, respectively. The compression strengths for 300 TEX, 600 TEX (warp density: 20 ends/cm), 600 TEX (warp density: 12 ends/cm), and 1200 TEX were 2.6 MPa, 3.8 MPa, 2.9 MPa, and 4.1 MPa, respectively.

Keywords: *3D woven, linear density, I-beam spacer fabric, flexural strength, compressive strength, the vacuum infusion process*

1. INTRODUCTION

The most significant load-carrying beams in the aircraft are the wing spars, designed to be reasonably robust to resist the loads and moments but also quite stiff to reduce wing bending under high stress. Hence, the spars in the wings were designed as structures with cross-sections similar to I-beams as laminated composites [1]–[3]. The most common failures on these laminated structures are delamination, buckling, and matrix-fiber cracking [4], [5]. To avoid such failures, novel strategies such as stitching, tufting, z-pinning [6], [7], and 3D weaving were studied by several researchers [8]–[10]. 3D woven composites are one of the most promising strategies that may create an alternative solution to improve the vulnerability of conventional laminates and ensuing local buckling failure under in-plane compression [11]–[14].

Parameters affecting 3D weaving should also be considered to achieve the potential of this novel process for advanced composite structures [15]–[18]. The linear density (TEX) of yarns formed from technical textiles brings load-carrying capability to the overall design; hence for weaving, the investigation of TEX is also one critical factor that needs to be studied. Eng et al. observed that fabrics with higher TEX enhanced the mechanical properties in 2D laminated structures through sharing the force effectively with more fibers [19]. Additionally, the effect of TEX was discussed with the crimp rate of the fiber, where the improvement was inversely related to the increase in TEX. Moreover, Asi has correlated the effect of TEX to void content in 2D composite structures. When the TEX was increased by 50%, the void content was also raised to 55.2% [20], with more interlacing points creating traps for voids during composite manufacturing. In addition, Liu and Hughes presented mechanical properties' dependency on varying weft density, warp density, and TEX. Hence, when the TEX of the

IBF: I-Beam Fabric
IBC: I-Beam Composite
LB-X: Load Bearing with X Vertical Wall

weft was increased more than eight times, two times increase in tensile strength was observed with more fibers that carry the load [21]. Aggarwal and Chatterjee investigated the influence of increasing the linear density of jute yarns up to 3 times on the static and dynamic properties of unidirectional jute yarn-reinforced epoxy composites. When the linear density of the yarn was doubled, there was an increase in tensile strength, impact strength, and storage modulus. However, as the linear density was increased by three times, a downward trend in these properties was observed [22]. Although several studies on the linear density effect for 2D laminated structures were performed, a lack of knowledge is still present in 3D composites.

In this study, the aim is to investigate the effect of TEX for 3D woven I-beam composites under flexural and compressive loading. Initially, 3D rectangular spacer fabrics were woven with E-glass fibers using a custom-built weaving machine. Then, 3D weaving with 300, 600, and 1200 TEX IBFs was extracted from the 3D woven, rectangular spacer fabric, followed by resin infusion to fabricate the IBCs. Since the composite manufacturing quality is directly related to the mechanical properties of the structures, a novel molding process is implemented. This approach involves an integration of a molding technique, specifically designed to enhance the uniform resin distribution and geometrical precision of an I-beam structure which is also customizable upon the geometry of the spacer fabric. This novel molding process ensures improved material integrity and, consequently, enhances the overall mechanical properties of the fabricated composites. Quality control measures are employed in conjunction with void content analysis through image processing of the IBCs further validating the effectiveness of this pioneering molding strategy. Thus, the void content of 300, 600, and 1200 TEX IBCs was found to be less than 6% for all specimens. The flexural and compressive strengths of all TEX IBCs were then investigated to define the effect of linear density considering both the change in the volume fraction of fibers and the composite manufacturing qualities. Moreover, the variation in warp and weft densities during weaving has created also an effect on the overall mechanical properties related to the cover factor for 600 and 1200 TEX IBCs. By increasing the cover factor for 600 TEX IBC from 25 to 34 through changing the warp when the weft is kept stable, a comparable compressive strength was achieved at 3.8 MPa to 1200 TEX IBC at 4.1 MPa even keeping the linear density low.

2. MATERIALS AND METHODS

2.1. Materials

Şişecam Elyaf supplied E-glass fibers at roving of 300, 600, and 1200 TEX linear densities. The weaving geometry was defined as spacer fabrics of glass fibers (GFs) in I-beam geometries. The weaving process was performed in a custom-built machine as shown in Figure S1.

2.2. Methods

2.2.1 Weaving I-beam fabrics with X vertical wall

Simultaneously four layers of weaving were performed with the required fabric length, flange width, and web height of the I-beam [23], [24]. The weaving process was detailed in the weaving plan and shown in Figure 1a and Figure *1*b, with black dots representing the wefts and colored lines showing the warps. The IBF's vertical wall (web) was employed through an “X” appearance with a connection point in the middle. This geometry will be named “Load Bearing with X vertical wall (LB-X), as shown in Figure *1*a. In multi-layer weavings such as IBCs, the weaving plan of each layer was prepared first. Two-ply weaving was required as one layer of fabric must be woven to form each flange (upper and lower) of the I-beam as shown in the 1st and 4th regions in Figure 1b. For the 2nd and 3rd regions where the vertical wall was formed, the weaving plan was changed as some of the warp groups in the upper and lower layers remained as floating yarns while the middle layers were woven. In the LB-X design, initially, the open form was woven as shown in Figure 1b, then the floating yarns were taken up from the fabric to form a vertical wall in a closed form as in Figure 1a. Afterward, the positions of the warps, represented by colored lines corresponding to the black-dotted wefts, were indicated. For the LB-X

IBF: I-Beam Fabric
IBC: I-Beam Composite
LB-X: Load Bearing with X Vertical Wall

design, where the weft is positioned over the warp, the cells are expressed in white in the lifting plan shown in Figure 1c.

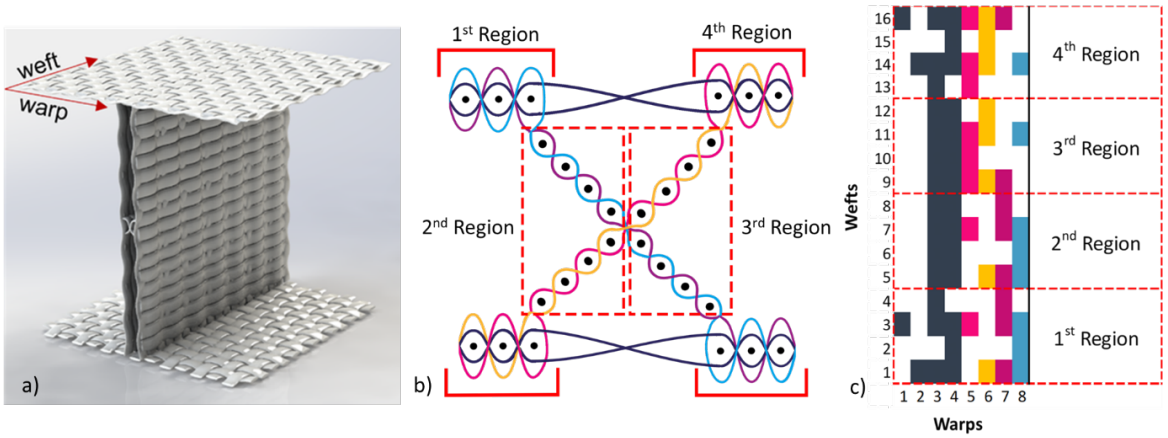

Figure 1: 3D woven I-beam spacer fabric, a) schematic view of LB-X design, b) open form of the weaving plan, and c) lifting plan of "Load Bearing with X vertical wall" (LB-X I-beam) used in the weaving machine.

Therefore, multiple IBFs were woven in a rectangular geometry, resulting in a cohesive structure as shown in Figure 2. Hence, I-beams were extracted from the rectangular fabric by conveniently cutting from the sides of vertical walls that will be molded separately for the vacuum infusion process, as well. For all IBCs, the effects of linear density were studied for 300, 600, and 1200 TEX IBFs. Since the warp and weft densities vary with the TEX of the GFs, the limitations for composite manufacturing were also considered. Hence, a smaller yarn width, such as 300 TEX, required an increase in warp density compared to 600 and 1200 TEX-based IBFs.

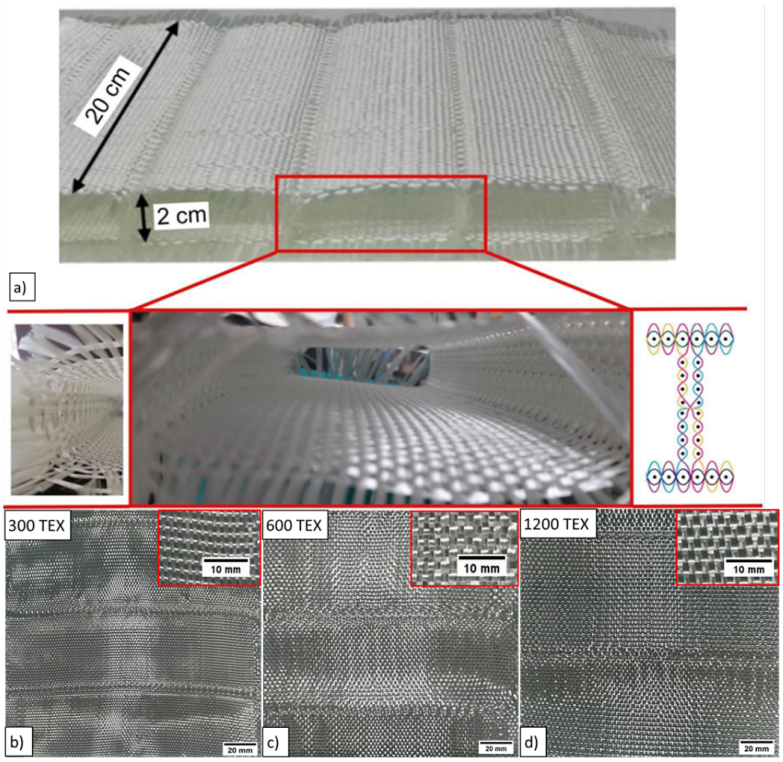

Figure 2: Multiple I-beam fabrics in a rectangular geometry, a) the view of LB-X vertical wall (left) and the weaving plan of LB-X vertical wall (right), b) top view of I-beam flanges woven by using GFs with 300, 600, and 1200 TEX linear densities.

IBF: I-Beam Fabric
IBC: I-Beam Composite
LB-X: Load Bearing with X Vertical Wall

During the weaving of 300 TEX, a warp density of 20 ends/cm with a weft density of 4 picks/cm provided the required dimensions. However, the warp densities for 600 and 1200 TEX were 12 ends/cm. To compare warp and weft densities on the cover factor and load-bearing capability of all 3D woven IBCs, 600 TEX were also produced to have a warp density of 20 ends/cm and a weft density of 4 picks/cm. The woven fabrics, which were then fabricated as composites, are presented in Table S1 in detail.

2.2.2 Fabrication and testing of IBCs

The IBCs with LB-X geometry on the vertical wall were fabricated with a custom-designed mold integrated VIP and shown in Figure S2. The mechanical properties of IBCs were investigated by applying both bending and compression tests for the TEX effect. The details of all fabricated IBCs are presented with the abbreviations and sample descriptions in Table S1. The flexural properties of IBCs were determined according to ASTM D790 by a 3-point bending test using SHIMADZU AGS-X 50 kN universal testing machine (UTM). Testing speed and the roller geometry are detailed in the Supplementary and shown in Figure S3. The compressive properties were tested in compliance with ASTM C365 to investigate the resistance of IBCs to out-of-plane forces.

3. RESULTS AND DISCUSSION

The mechanical properties of composites are highly correlated with the production quality since voids may create discontinuities and serve as stress raisers [25]. Besides the novel manufacturing approaches implemented here to fabricate high-quality hollow beam structures, the void content analysis was also performed. The optical microscopy images were initially taken from the IBCs and then studied by image processing software for upper, lower, and vertical wall surfaces. Since the shearing effect will dominate the web, the vertical wall's void content is primarily discussed. The void content of IBCs vertical walls with 300, 600, and 1200 TEX is shown in Figure 3 with an average value of 4.5%, 5.6%, and 0.8%, respectively. The sharp decrease in 1200 TEX was attributed to improved quality through a better resin flow with enhanced linear density as opposed to earlier reported 2D laminated structures where transverse resin flow is dominated by the capillary effect. The void content of the upper and lower flanges is also calculated with a similar approach and presented in Table S2. A similar trend has been observed for 1200 TEX samples as of creating more capillary lines with increasing fiber content but the dominating behavior has been more clear on the vertical walls as of 3D structures. All the void analyses did not demonstrate a significant difference when different warp densities as 20 ends/cm and 12 ends/cm of 600 TEX, were considered. Hence the reported value for 600 TEX of 12:4 warp-to-weft ratio was discussed.

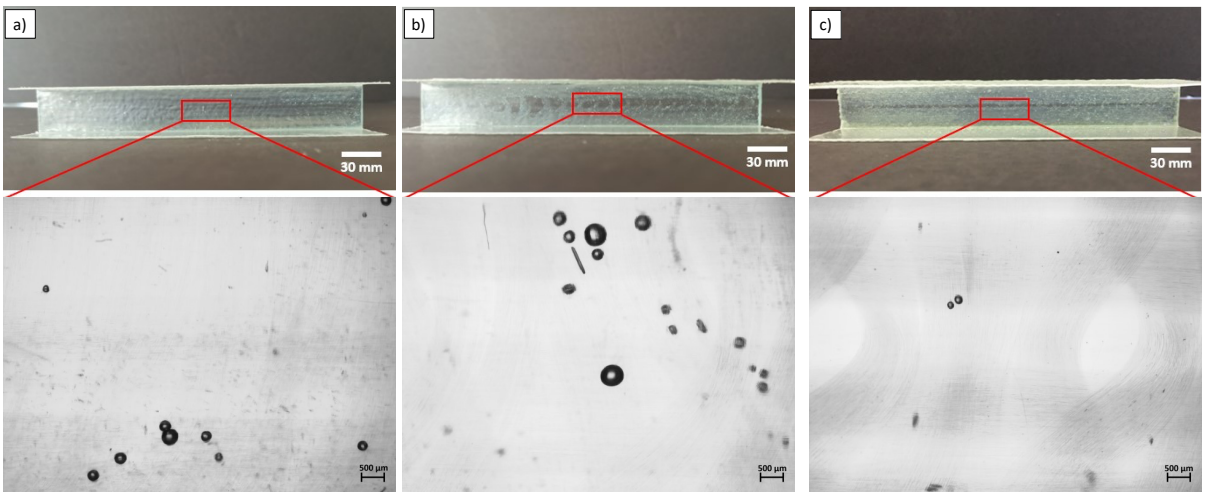

Figure 3: Optical microscope images of the manufactured woven I-beam composites at the vertical wall of a) IBC-300, b) IBC-600, c) IBC-1200.

IBF: I-Beam Fabric
IBC: I-Beam Composite
LB-X: Load Bearing with X Vertical Wall

Cover factor, an indicator of the looseness or tightness of the fabric, establishes a comparison of the relative proximity of yarns and indicates how much the weft fills the fabric in the warp direction. Especially when the fabric architecture is altered, the specific needs for mechanical requirements can be met through several parametric studies. The calculation of cover factor for 300, 600, and 1200 TEX fabrics in IBCs per unit area was explained in detail in Supplementary Information. Typically, in the vertical wall, the warps act as load carriers; hence the warp density is considered the dominant feature within this region. The highest cover factor achieved in the warp direction was 24.5, as in 600 TEX (20:4), with a total cover factor of 34.3, as presented in Table 1. Several studies from earlier reports established the correlation between the shear rigidity of fabrics to parameters such as cover factor and yarn density [26], [27] emphasizing an enhanced shear rigidity with the cover factor. Along with these studies, the cover factor effect on the load-bearing capacity is also discussed within the 3D woven composites for compression and bending loadings.

Table 1: The cover factors for warp and weft densities of 300, 600, and 1200 TEX IBCs.

TEX	Warp Density (ends/cm)	Weft Density (picks/cm)	Cover Factor Warp Direction	Cover Factor Weft Direction	Total Cover Factor
300	20	4	17.3	6.9	24.2
600	12	4	14.7	9.8	24.5
600	20	4	24.5	9.8	34.3
1200	12	4	20.8	13.9	34.6

The flexural properties of IBCs were studied by 3-point bending tests, and calculations were performed accordingly. During 3-point bending, the matrix fractures were observed at the contact points of the upper pins on the IBCs, followed by higher strains at the lower flange under tension. The radial cracks were initiated to the web from the lower flange and then merged to matrix cracks occurring from the upper flanges and finally failed at the middle of the X region, as shown in Figure 4a. The typical load-displacement curves exhibited an initial linear portion for all specimens and were followed by an increase till a slight reduction with a kink in the curve. The results demonstrated that the maximum load-carrying capacity was achieved when 600 TEX (warp density: 20 ends/cm) was employed in IBCs, as shown in Figure 4c. The main reason for this was mainly the highest cover factor supporting the structure to achieve the shear rigidity, followed by 1200 TEX IBCs at similar fiber volume fractions. The first ply crack failure for 600 TEX with 12 ends/cm warp density resulted in a higher strain due to the lower cover factor that drives the structure to buckle. However, within the increase in the cover factor, a more brittle behavior with the lowest strain for first-ply failure is observed for IBC-600-20. Additionally, the highest peak load was also achieved for IBC-600-20 after the first peak load due to the stiffening effect seen in the plastic region. All the results are presented in Table 2.

Table 2: 3-point bending test results of 300 TEX, 600 TEX, and 1200 TEX IBCs.

Sample Code	Max. Flexural Stress (MPa)	Max. Flexural Strain (mm/mm)	First Ply Crack (MPa)	Strain of First Ply Crack (mm/mm)	Max. Flexural Load (N)	Max. Deflection (mm)
IBC-300-20	8.6	0.012	6.2	0.0044	2451	5.3
IBC-600-20	9.2	0.020	6.7	0.0028	3405	8.1
IBC-600-12	8.5	0.012	8.2	0.0088	2693	5.0
IBC-1200-12	8.8	0.011	5.4	0.0036	3145	4.6

Moreover, compression tests performed on all IBCs revealed two ways of failure behavior. The first failure happened by breaking from the intersection of the flange to the web where the accumulation of voids at the corner was prominent or failed at the X region on the vertical wall where no significant voids were present, as shown in Figure 4b. Under compressive loads, the deformation is initially linear, followed by a peak load, and finally, a dramatic drop due to the buckling of the vertical wall. The stress-

strain plots relating the TEX effect and cover factor under compression are shown in Figure 4d. The data mainly presented similar characteristics in the two regions by covering factors below 25 and above 34, indicating comparable load-carrying capabilities related to fiber content. In IBC-300-20 and IBC-600-12, a lower fiber content was present compared to samples with IBC-1200-12 and IBC-600-20. Hence the compressive stress of IBC-1200-12 and IBC-600-20 were 4.1 and 3.8 MPa, respectively. However, IBC-300-20 and IBC-600-12 exhibited compressive stress of 2.6 and 2.9 MPa below the cover factor of 25. Additionally, at higher strains, when the cover factor was below 25, with fewer fibers resisting compression, buckling behavior was observed in a ductile fashion, as expected.

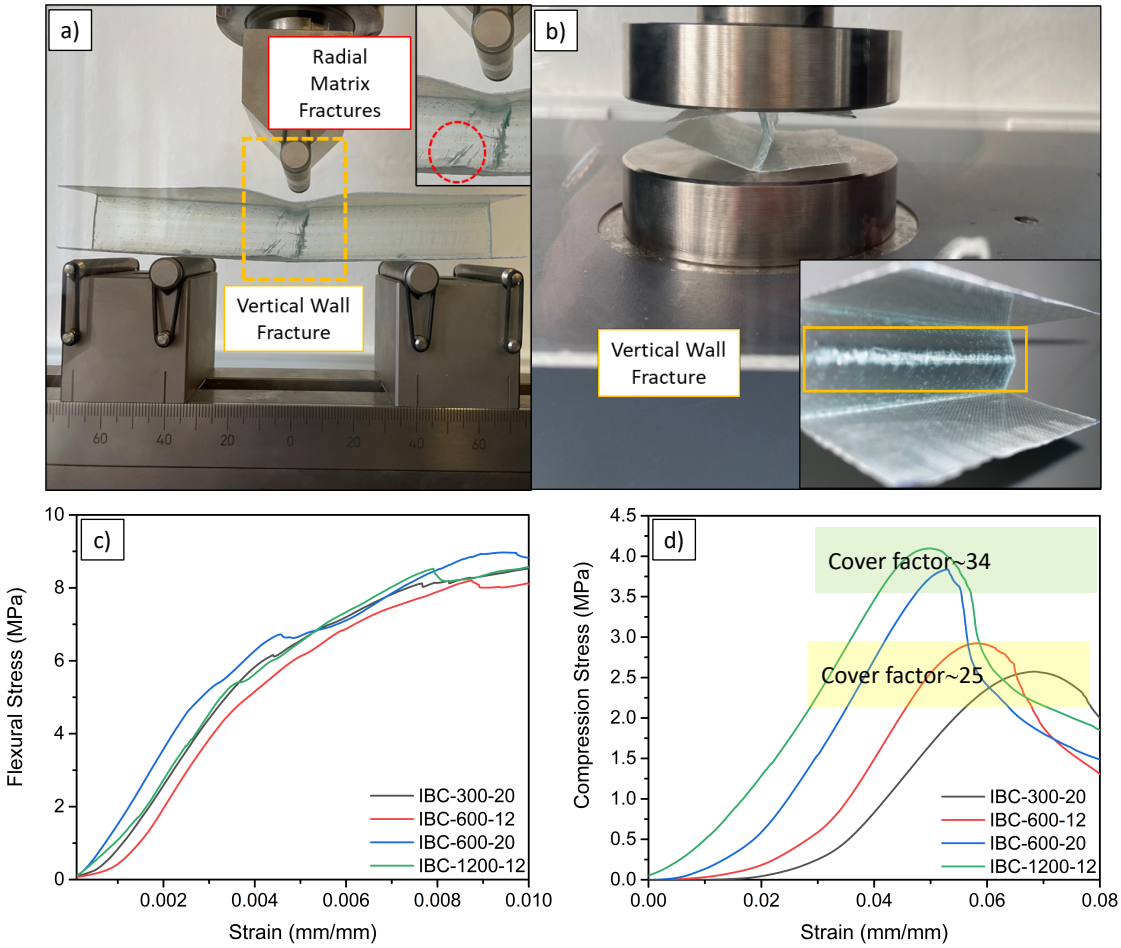

Figure 4: a) 3-point bending test of an IBC-600-20 with a zoomed inset of vertical wall and flange during fracture, b) compression test of an IBC-1200-12 with vertical wall fractures at X region, c) flexural stress-strain plots of IBCs, d) compression stress-strain plots of IBCs.

4. CONCLUSION

In this study, 3D woven I-beam fabrics and I-beam composites have been fabricated with custom-built weaving instrumentation. The effect of TEX and fabric cover on the flexural and compressive strength were studied for all I-beam composites. Since increasing the TEX from 300 to 1200 directly affects the fiber content, the TEX and yarn density on the cover factor have been investigated in detail. To the best of our knowledge, this is the first study establishing the correlation of yarn density or TEX to the load-carrying capability of 3D woven spacer fabrics as a potential candidate for structural applications. When increasing the warp density from 12 ends/cm to 20 ends/cm at constant weft density, IBC-600-12 and IBC-600-20 showed a cover factor of 25 and 34, respectively. Since the cover factor is increased upon the enhancement in warp density, the flexural properties were in a similar trend showing the highest maximum force carrying capability of 3405 N; however, compromising on the first ply strain which is related to higher fiber content. Comparing the lower TEX composites, as in IBC-300-20 to IBC-

IBF: I-Beam Fabric
IBC: I-Beam Composite
LB-X: Load Bearing with X Vertical Wall

600-20, the cover factor was decreased to 25, and the lowest achievable load-carrying capacity was observed among all IBCs. Moreover, due to fewer fibers, the IBC-300-20 exhibited a higher first-ply failure resulting in a buckling of the structure. On the contrary, no buckling was observed when IBC-1200-12 was studied. In compression tests, the results were directly related to the cover factor showing compressive stress of IBC-1200-12 and IBC-600-20 as 4.1 and 3.8 MPa, respectively. However, IBC-300-20 and IBC-600-12 exhibited compressive stress of 2.6 and 2.9 MPa below the cover factor of 25.

ACKNOWLEDGEMENT

This study was funded by the Scientific and Technological Research Council of Turkey (TUBITAK; project number 218M703 (218M704)), 1003 Primary Subjects R&D Funding Program, and ITU BAP project number: 40738. We would like to thank Şişecam Elyaf for the glass fiber supply. We would like to thank Suat Ebil for his technical contribution to composites manufacturing.

REFERENCES

[1] S. Gudmundsson, "Aircraft Structural Layout," *General Aviation Aircraft Design*, pp. 97–131, Jan. 2014, doi: 10.1016/b978-0-12-397308-5.00005-2.

[2] S. Kamle, R. Kitey, P. M. Mohite, C. S. Upadhyay, C. Venkatesan, and D. Yadav, "Design of Aircraft Structures: An Overview," pp. 231–250, 2017, doi: 10.1007/978-981-10-2143-5_12.

[3] V. G. P. S, R. Chandan, and H. A. Shivappa, "Structural Analysis and Optimization for Spar Beam of an Aircraft," *International Research Journal of Engineering and Technology(IRJET)*, vol. 4, no. 9, pp. 994–998, 2017, [Online]. Available: https://irjet.net/archives/V4/i9/IRJET-V4I9175.pdf

[4] M. R. Wisnom, "The role of delamination in failure of fibre-reinforced composites," *Philosophical Transactions of the Royal Society A: Mathematical, Physical and Engineering Sciences*, vol. 370, no. 1965, pp. 1850–1870, 2012, doi: 10.1098/rsta.2011.0441.

[5] R. Talreja and C. V. Singh, *Damage and failure of composite materials*. 2012. doi: 10.1017/CBO9781139016063.

[6] I. Gnaba, X. Legrand, P. Wang, and D. Soulat, "Through-the-thickness reinforcement for composite structures: A review," *Journal of Industrial Textiles*, vol. 49, no. 1, pp. 71–96, 2019, doi: 10.1177/1528083718772299.

[7] Y. S. Perera, R. M. H. W. Muwanwella, P. R. Fernando, S. K. Fernando, and T. S. S. Jayawardana, *Evolution of 3D weaving and 3D woven fabric structures*, vol. 8, no. 1. Springer Singapore, 2021. doi: 10.1186/s40691-020-00240-7.

[8] P. Schegner, M. Fazeli, C. Sennewald, G. Hoffmann, and C. Cherif, "Technology Development for Direct Weaving of Complex 3D Nodal Structures," *Applied Composite Materials*, vol. 26, no. 1, pp. 423–432, 2019, doi: 10.1007/s10443-018-9734-9.

[9] R. K. Mishra, M. Petru, B. K. Behera, and P. K. Behera, "3D Woven Textile Structural Polymer Composites: Effect of Resin Processing Parameters on Mechanical Performance," *Polymers (Basel)*, vol. 14, no. 6, Mar. 2022, doi: 10.3390/polym14061134.

[10] Z. Kamble, R. K. Mishra, B. K. Behera, M. Tichý, V. Kolář, and M. Müller, "Design, development, and characterization of advanced textile structural hollow composites," *Polymers*, vol. 13, no. 20. 2021. doi: 10.3390/polym13203535.

IBF: I-Beam Fabric
IBC: I-Beam Composite
LB-X: Load Bearing with X Vertical Wall

[11] F. Turgut, A. Koycu, H. Cebeci, G. Neje, B. K. Behera, and E. Ozden-Yenigun, “Hierarchical cnts grown multifunctional 3d woven composite beams for aerospace applications,” *AIAA Scitech 2020 Forum*, vol. 1 PartF, no. January, 2020, doi: 10.2514/6.2020-0153.

[12] B. N. Cox, M. S. Dadkhah, W. L. Morris, and J. G. Flintoff, “Failure mechanisms of 3D woven composites in tension, compression, and bending,” *Acta Metallurgica Et Materialia*, vol. 42, no. 12, pp. 3967–3984, 1994, doi: 10.1016/0956-7151(94)90174-0.

[13] A. P. Mouritz, M. K. Bannister, P. J. Falzon, and K. H. Leong, “Review of applications for advanced three-dimensional fibre textile composites,” *Compos Part A Appl Sci Manuf*, vol. 30, no. 12, pp. 1445–1461, 1999, doi: 10.1016/S1359-835X(99)00034-2.

[14] E. J. Pineda, B. A. Bednarcyk, T. M. Ricks, B. Farrokh, and W. Jackson, “Multiscale failure analysis of a 3D woven composite containing manufacturing induced voids and disbonds,” *Compos Part A Appl Sci Manuf*, vol. 156, no. February, p. 106844, 2022, doi: 10.1016/j.compositesa.2022.106844.

[15] A. R. Horrocks and S. C. Anand, *Handbook of Technical Textiles: Second Edition*, vol. 1. Woodhead Publishing, 2015. doi: 10.1016/C2015-0-01011-5.

[16] X. Chen, *Advances in 3D Textiles*. 2015. doi: 10.1016/c2013-0-16485-9.

[17] M. P. Bin Saiman, M. S. Bin Wahab, and M. U. Bin Wahit, “The effect of yarn linear density on mechanical properties of plain woven kenaf reinforced unsaturated polyester composite,” *Applied Mechanics and Materials*, vol. 465–466, no. December, pp. 962–966, 2014, doi: 10.4028/www.scientific.net/AMM.465-466.962.

[18] M. Dahale *et al.*, “Effect of weave parameters on the mechanical properties of 3D woven glass composites,” *Compos Struct*, vol. 223, no. October 2018, p. 110947, 2019, doi: 10.1016/j.compstruct.2019.110947.

[19] K. M. Eng, M. Mariatti, N. R. Wagiman, and K. S. Beh, “Effect of different woven linear densities on the properties of polymer composites,” *Journal of Reinforced Plastics and Composites*, vol. 25, no. 13, pp. 1375–1383, 2006, doi: 10.1177/0731684406065081.

[20] O. Asi, “Effect of different woven linear densities on the bearing strength behaviour of glass fiber reinforced epoxy composites pinned joints,” *Compos Struct*, vol. 90, no. 1, pp. 43–52, 2009, doi: 10.1016/j.compstruct.2009.01.007.

[21] Q. Liu and M. Hughes, “The fracture behaviour and toughness of woven flax fibre reinforced epoxy composites,” *Compos Part A Appl Sci Manuf*, vol. 39, no. 10, pp. 1644–1652, 2008, doi: 10.1016/j.compositesa.2008.07.008.

[22] M. Aggarwal and A. Chatterjee, “Effect of Yarn Linear Density on Static and Dynamic Mechanical Properties of Jute Yarn Reinforced Epoxy Composites,” *Journal of The Institution of Engineers (India): Series E*, vol. 104, no. 1, pp. 73–81, Jun. 2023, doi: 10.1007/s40034-023-00266-8.

[23] X. Chen, *Hollow three-dimensional woven fabrics*, no. 2004. Elsevier Ltd., 2015. doi: 10.1016/B978-1-78242-214-3.00003-6.

[24] G. Neje and B. K. Behera, “Influence of cell geometrical parameters on the mechanical properties of 3D integrally woven spacer sandwich composites,” *Compos B Eng*, vol. 182, no. November 2019, p. 107659, 2020, doi: 10.1016/j.compositesb.2019.107659.

[25] D. Hull and T. W. Clyne, “An Introduction to Composite Materials,” *An Introduction to Composite Materials*, 1996, doi: 10.1017/cbo9781139170130.

[26] B. Behera and P. Hari, *Woven Textile Structure: Theory and Applications*. Woodhead Publishing, 2016. doi: 10.1016/b978-0-08-100407-4.09001-3.

[27] F. Wang, G. xu, and B. xu, “Predicting the Shearing Rigidity of Woven Fabrics,” *Textile Research Journal*, vol. 75, no. 1, pp. 30–34, 2005, doi: 10.1177/004051750507500106.